AGU PUBLICATIONS

Geophysical Research Letters

RESEARCH LETTER

10.1002/2014GL062406

Key Points:
- ECH waves can trap upflowing electrons in the magnetosphere
- ECH waves accelerate electrons to keV energies and form butterfly distributions
- ECH waves provide a low-energy electron source for the radiation belts

Correspondence to:
R. B. Horne,
R.Horne@bas.ac.uk

Citation:
Horne, R. B. (2015), Trapping and acceleration of upflowing ionospheric electrons in the magnetosphere by electrostatic electron cyclotron harmonic waves, *Geophys. Res. Lett.*, *42*, 975–980, doi:10.1002/2014GL062406.

Received 1 NOV 2014
Accepted 23 JAN 2015
Accepted article online 27 JAN 2015
Published online 24 FEB 2015

Trapping and acceleration of upflowing ionospheric electrons in the magnetosphere by electrostatic electron cyclotron harmonic waves

Richard B. Horne[1]

[1]British Antarctic Survey, Cambridge, UK

Abstract During geomagnetically active conditions upflowing field-aligned electrons which form part of the Birkland current system have been observed at energies of up to 100 eV. If the first adiabatic invariant is conserved, these electrons would reach the conjugate ionosphere without trapping in the magnetosphere. Here we show, by using quasi-linear diffusion theory, that electrostatic electron cyclotron harmonic (ECH) waves can diffuse these low-energy electrons in pitch angle via Doppler-shifted cyclotron resonance and trap them in the magnetosphere. We show that energy diffusion is comparable to pitch angle diffusion up to energies of a few keV. We suggest that ECH waves trap ionospheric electrons in the magnetosphere and accelerate them to produce butterfly pitch angle distributions at energies of up to a few keV. We suggest that ECH waves play a role in magnetosphere-ionosphere coupling and help provide the source electron population for the radiation belts.

1. Introduction

Upflowing field-aligned electrons of energies up to a hundred eV or so have been observed on high-latitude field lines [*Lin et al.*, 1979; *Cattell et al.*, 2004]. These field-aligned flows are part of the region 1 and 2 current systems that couple the magnetosphere to the ionosphere [*Iijima and Potemra*, 1978] and intensify during geomagnetically active conditions [*Anderson et al.*, 2008]. As electrons flow upward along the magnetic field, the angular width of the distribution becomes very narrow if the first adiabatic invariant is conserved and the electrons would be confined to the loss cone. In the absence of any scattering these electrons would reach the conjugate ionosphere without trapping in the magnetosphere, assuming that the field lines are closed on the Earth. Near the geomagnetic equator, narrow field-aligned electron "beams" have been observed at energies up to 100 eV [*Abel et al.*, 2002a, 2002b]. Equatorial observations show that these field-aligned beams tend to evolve in time to become broader in pitch angle and energized up to energies of a few keV at large pitch angles. Not all field-aligned distributions show this time evolution but most do. It has been suggested that this time evolution is due to scattering by wave-particle interactions, but the type of waves responsible remains an open question.

Upflowing electron beams can excite a variety of different plasma waves. They have been associated with the generation of upgoing auroral hiss via Landau resonance [*Lin et al.*, 1984] and electron acoustic waves [*Tokar and Gary*, 1984]. Both types of waves have a large electrostatic component. Upgoing hiss is usually observed at relatively high latitudes and therefore cannot cause electron diffusion to large equatorial pitch angles approaching 90°. To diffuse electrons to large equatorial pitch angles, wave scattering near the geomagnetic equator is required.

In the magnetosphere there are several types of plasma waves which are observed near the magnetic equator. However, they are not usually associated with an electron beam. A necessary condition for beam-plasma wave excitation is that there should be a positive gradient in the velocity distribution function $\partial f(v)/\partial v_{\|} > 0$. While a positive gradient has been found in low-altitude observations [*Lin et al.*, 1979] the beams referred to in the equatorial observations are not actually beams but are in fact a peak in the differential energy flux (DEF) [*Abel et al.*, 2002a, 2002b]. Since $f(v)$ is proportional to DEF$/E^2$ a peak in the DEF does not mean that $\partial f(v)/\partial v_{\|} > 0$ or that the plasma is unstable to beam-generated waves. Therefore, although we do not rule out beam-generated waves here, we consider pitch angle scattering by other nonbeam-driven waves which are more commonly observed.

Some of the most important wave emissions that can diffuse electrons near the equator include plasmaspheric hiss, chorus waves, magnetosonic waves, electromagnetic ion cyclotron (EMIC), and electrostatic electron cyclotron harmonic (ECH) waves. These waves could cause effective electron diffusion if they satisfy the Doppler-shifted cyclotron resonance condition which can be written as

$$v_{\parallel} = \frac{\omega}{k_{\parallel}}\left(1 - \frac{n\Omega_q}{\gamma\omega}\right) \quad (1)$$

where ω is the wave frequency, Ω_q is the cyclotron frequency for each species q, n is the harmonic number, $k_{\parallel}$ and $v_{\parallel}$ are the k vector and particle velocity parallel to the background magnetic field direction, and γ is the relativistic correction factor. The resonance condition shows that for small pitch angles the resonant energy can become very low either when the parallel phase velocity is small, or when wave frequency becomes close to $n\Omega_q$. For whistler mode waves the parallel phase velocity is a minimum just inside the high-density plasmapause but the frequency of waves such as plasmaspheric hiss which are observed in that region is usually so low that the resonant energy is typically >100 keV [*Meredith et al.*, 2004]. Chorus waves are usually observed outside the plasmasphere where the frequency is higher but the density is lower, and as a result the resonant energy is usually >1 keV for lower band waves and >100 eV for upper band waves [*Thorne et al.*, 2010]. Magnetosonic waves usually have frequencies below the local lower hybrid resonance frequency so that the lowest resonant energy is from Landau resonance and is typically a few tens of keV [*Horne et al.*, 2007]. EMIC waves have frequencies below the proton cyclotron frequency and tend to resonate with much higher energy electrons >500 keV. However, ECH waves are observed with frequencies from typically $(n + 0.1)\Omega_e$ to $(n + 0.9)\Omega_e$ [*Horne et al.*, 1981; *Paranicas et al.*, 1992; *Ni et al.*, 2011] and can resonate with low-energy electrons <100 eV. These waves are usually associated with electron precipitation of 1–10 keV electrons responsible for the diffuse aurora [*Kennel et al.*, 1970; *Thorne et al.*, 2010]. However, here we examine whether ECH waves could trap and accelerate much lower energy upflowing ionospheric electrons in the magnetosphere by calculating pitch angle and energy diffusion rates.

2. ECH Growth Rates

In order to calculate the diffusion rates it is first necessary to calculate the resonant wave numbers. There is no simple way to do this other than to calculate the dispersion relation numerically. Several studies have shown that to obtain the essential features of ECH waves two or more plasma components are required [*Hubbard and Birmingham*, 1978; *Ashour-Abdalla and Kennel*, 1978; *Rönnmark and Christiansen*, 1981; *Horne et al.*, 1981]. They include a hot component which drives the instability via a loss cone distribution and a cold component. The cold component determines the dispersion of the waves at the resonant wave numbers and the number of harmonic bands that can be excited. Here we have adopted the model used previously [*Horne and Thorne*, 2000] which has a hot component with a temperature of 1 keV and density $n_h = 5 \times 10^5$ m^{-3} and a cold component with temperature of 1 eV and density $n_c = 10^6$ m^{-3}. The loss cone is represented by a "subtracted Maxwellian" component with parameters $\beta = 0.02$ and $\Delta = 0.5$ which represent the width and depth of the loss cone, respectively. For more details see *Ashour-Abdalla and Kennel* [1978]. The only source of instability is the loss cone which is restricted to very small pitch angles. No temperature anisotropy is present in the distribution. To represent conditions near $L = 7$, the electron gyrofrequency is $f_{ce} = |\Omega_e|/(2\pi) = 2.54$ kHz and the upper hybrid resonance frequency is $f_{UHR}/f_{ce} = 4.45$. The electron gyroradius (ρ) is 37.22 m.

Using the dispersion solver in the HOTRAY code [*Horne*, 1989], Figure 1 shows the spatial growth rates as a function of frequency for a propagation angle of $\psi = 89.5°$ with respect to the magnetic field direction. ECH waves can be excited up to and including the sixth harmonic band which is well above the band containing f_{UHR}. Note also that below f_{UHR} wave growth tends to be in the upper half of each band, whereas above f_{UHR} wave growth tends to be in the lower half. This type of frequency banding is characteristic of ECH waves observed in the early morning through dawn to the dayside at geosynchronous orbit [*Hubbard and Birmingham*, 1978]. ECH waves are often used to determine f_{UHR} and hence the plasma density. This is very difficult in practice, but the results here suggest that it is better to determine f_{UHR} from the band with maximum wave amplitude rather than the highest-frequency band.

At night ECH waves are often observed at very low frequencies near $1.1f_{ce}$. Figure 1 (bottom) shows an example representing these waves where the cold electron density has been reduced to $n_c = 3 \times 10^4$ m^{-3}.

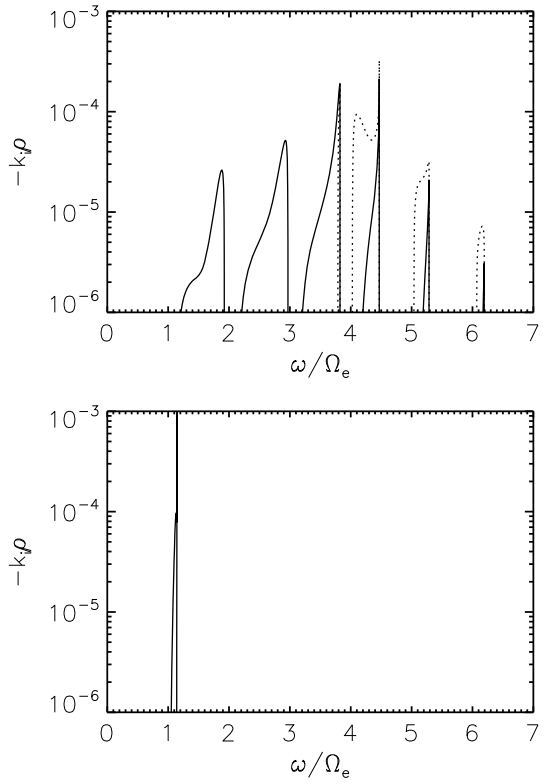

Figure 1. Spatial growth rates of ECH waves as a function of normalized frequency. The dotted lines are growth rates where the group velocity perpendicular to the magnetic field is positive. The cold plasma density is (top) $n_c = 10^6$ m^{-3} and (bottom) 3×10^4 m^{-3}.

Wave growth is present near $1.1f_{ce}$. The low cold plasma density changes wave dispersion in the higher bands such that the frequency becomes very close to the cyclotron harmonics at the resonant wave numbers and so from equation (1) $v_{\parallel}$ is very small and cyclotron damping prevents growth in the higher bands. Note that in this case $f_{UHR}/f_{ce} = 2.76$ but growth is only possible at much lower frequencies. These two cases enable us to examine the effects of wave frequency on the diffusion rates.

3. Electron Diffusion Rates

To calculate the electrostatic electron diffusion rates, we have used the formulation of *Lyons* [1974] and *Horne and Thorne* [2000]. The electric field spectrum is assumed to have a Gaussian form with spread of wave normal angles $\Delta\psi = 0.5°$ centered on resonant parallel $k_{\parallel 0}$ and perpendicular $k_{\perp 0}$ wave numbers. The $k_{\perp 0}$ were determined from the frequency of maximum spatial growth rate (Figure 1) in each band for $\psi = 89.5°$ which then define $k_{\parallel 0}$. Since the amplitude of ECH waves associated with substorms is typically >1 mV m^{-1} [*Meredith et al.*, 2000] bounce-averaged diffusion rates were calculated assuming a wave amplitude of 1 mV m^{-1} for waves in each of the first five bands and therefore should underestimate rather than overestimate the rate of diffusion. The formulation is exactly the same as that given in *Horne and Thorne* [2000] except here we also include energy diffusion and extend the calculations to lower energies.

Figure 2 shows the bounce-averaged pitch angle $\langle D_{\alpha\alpha}\rangle$ and energy $\langle D_{EE}\rangle$ diffusion rates for selected electron energies. The diffusion rates are for waves in the first five harmonic bands. At low energies (10 eV) pitch angle diffusion is restricted to regions outside the loss cone which is approximately 3° at this location ($L = 7$). However, between 50 eV and 1 keV diffusion at the edge of the loss cone becomes much higher and exceeds 8.4×10^{-5} s^{-1}. This value is very significant as it corresponds to the strong diffusion rate for ~100 eV electrons assuming an albedo of 25% due to electron backscatter from the atmosphere. *Ni et al.* [2011] also found that ECH waves can approach the strong diffusion rate near 200 keV based on more detailed modeling of data, although their diffusion rates were a little smaller, due to differences in the wave properties. Strong diffusion is usually associated with pitch angle scattering into the loss cone, but in the case we are considering here, the loss cone would be filled by upflowing electrons from the ionosphere. Observations show that between 50 and 100 eV the electron distribution inside the loss cone is indeed higher than that at larger pitch angles at the same energy [*Abel et al.*, 2002a]. Since pitch angle diffusion extends to 60° or more electrons will be diffused out of the loss cone to larger pitch angles very effectively by ECH waves. The electrons would then mirror above the ionosphere and become trapped inside the magnetosphere.

We emphasize that the ECH waves are assumed to be generated by the diffusion of electrons into the loss cone. When upflowing electrons from an ionospheric source reach the equatorial region, the loss cone at low energies becomes filled but the loss cone at higher energies (few keV) may remain empty or partially filled. Since resonance extends over a range of energies and since the resonant energy changes as the waves propagate, the waves may continue to grow on the higher energy part of the loss cone but act to diffuse electrons out of the loss cone at lower energies, provided at lower energies the phase space density inside the loss cone is larger than that outside.

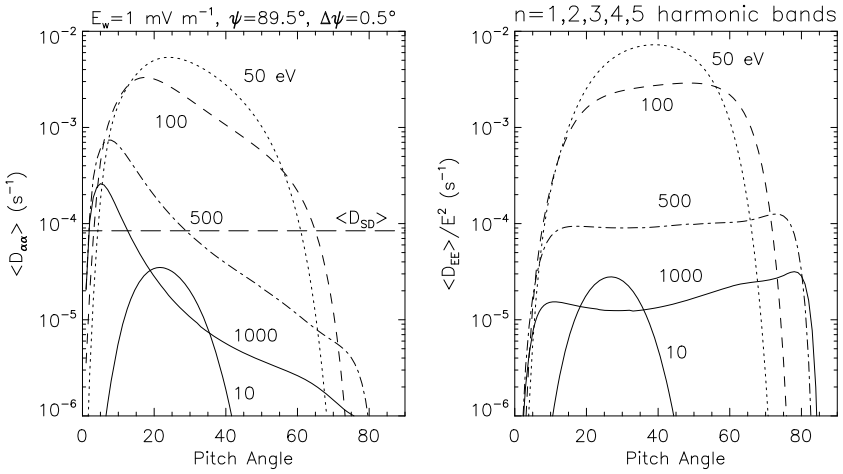

Figure 2. (left) Bounce-averaged pitch angle and (right) energy diffusion rates as a function of equatorial pitch angle for selected energies. The strong diffusion rate for 100 eV electrons is approximately 8.4×10^{-5} s^{-1}.

One of the most striking results shown in Figure 2 is that energy diffusion is comparable to pitch angle diffusion at each energy. Energy diffusion even exceeds pitch angle diffusion for pitch angles >40° and extends up to 70°–80°. Thus, for a distribution that is peaked in the field-aligned direction at low energies, ECH waves not only diffuse electrons to larger pitch angles but also accelerate them rapidly to higher energies. It is difficult to estimate the timescale for this to occur since diffusion depends on the gradients in the distribution function as well as the diffusion coefficients. However, by using the inverse of the diffusion rate, one may estimate a timescale of 5–15 min for wave amplitudes of 1 mV m^{-1} or so. This corresponds well to the evolution field-aligned distributions observed by *Abel et al.* [2002a, 2002b].

Diffusion rates for the low-density case corresponding to ECH waves near $1.1f_{ce}$ are shown in Figure 3. In this case pitch angle diffusion is again very important and can exceed the strong diffusion rate. It also extends across the loss cone. Thus, lower frequency waves can also diffuse electrons out of the field-aligned flow and trap them in the magnetosphere. However, energy diffusion appears to maximize near 500 eV. This is due to the large reduction in plasma density which reduces the frequency of the waves and significantly increases the resonant wave number. Thus, it seems that lower frequency ECH waves are less effective in accelerating electrons than the more common multiband ECH waves. Since waves near $1.1f_{ce}$ are usually observed near local midnight, whereas the multiharmonic waves are observed near dawn and across the dayside magnetosphere, this suggests that there could be a significant difference in the shape of the electron distribution at energies of 50 to a few hundred eV with local time.

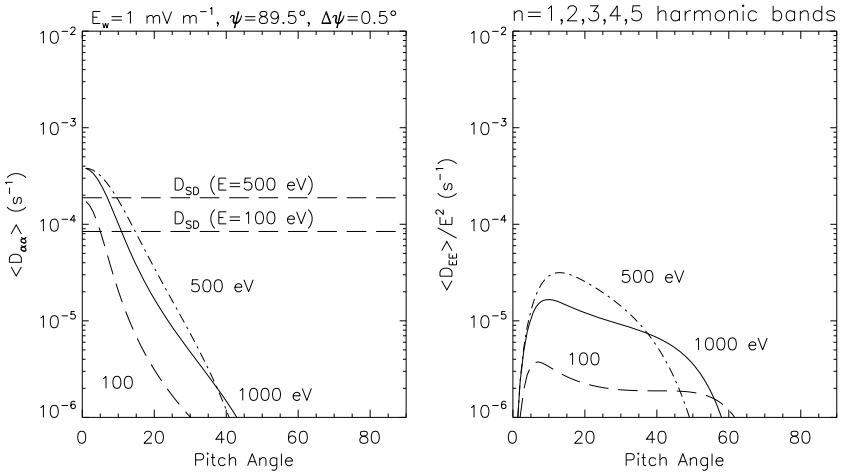

Figure 3. Same as Figure 2 but for ECH waves at $1.1f_{ce}$ corresponding to very low cold plasma density as shown in Figure 1 (bottom).

4. Butterfly Distributions

It is interesting to consider the shape of the pitch angle distribution that would result from ECH wave diffusion. Assuming a field-aligned flow at energies of 100 eV or so and assuming a loss cone at higher energies and a distribution that falls with increasing energy, one might expect the distribution at 50–100 eV to first broaden in pitch angle. Between 500 eV and a few keV energy diffusion exceeds pitch angle diffusion for $\alpha > 40°$, and thus, one might expect electrons to diffuse to higher energy. Under these circumstances the electron distribution would exhibit a butterfly-type distribution peaked at intermediate pitch angles between 20° and 60° and between a few hundred eV and a few keV where the peak moves to larger pitch angles with increasing energy. Such butterfly distributions have been observed at the Earth by the CRRES satellite (but not published) and at Saturn [*Rymer et al.*, 2008]. At Saturn it has been suggested that butterfly distributions are due to a recirculation transport process, but since ECH waves are also observed at Saturn, it may be possible that they are due to diffusion by ECH waves as discussed above.

5. Conclusions

We have calculated electron diffusion rates due to electrostatic ECH waves characteristic of those found near-geosynchronous orbit and assessed their impact on upflowing ionospheric electrons. We find the following results:

1. For energies of 50–100 eV electron pitch angle and energy diffusion rates are comparable and extend from the loss cone to larger pitch angles. Energy diffusion can exceed pitch angle diffusion at larger pitch angles. This suggests that ECH waves can diffuse 50–100 eV electrons out of a field-aligned flow to larger pitch angles and accelerate them to energies of a few keV.
2. The resulting pitch angle distribution should develop into a butterfly distribution with a peak at pitch angles between 20° and 60° where the peak appears at larger pitch angles with increasing energy. Since ECH waves are observed at Earth, Jupiter, and Saturn, we suggest that they contribute to the formation of butterfly pitch angle distributions at these three planets.
3. While dayside and nightside ECH waves can trap electrons in the magnetosphere, multiharmonic dayside waves are more effective in accelerating electrons to keV energies.

We suggest that ECH waves play a role in magnetosphere-ionosphere coupling by trapping upflowing electrons in the magnetosphere and that they help to provide an internal source electron population of a few keV for further acceleration to radiation belt energies.

Acknowledgments
The research leading to these results has received funding from the European Union Seventh Framework Programme (FP7/2007-2013) under grant agreement 606716 SPACESTORM, STFC grant ST/I001727/1, and the Natural Environment Research Council.

The Editor thanks Mary Hudson and S. Gary for their assistance evaluating this paper.

References

Abel, G. A., A. N. Fazakerley, and A. D. Johnstone (2002a), Simultaneous acceleration and pitch angle scattering of field-aligned electrons observed by the LEPA on CRRES, *J. Geophys. Res.*, *107*(A12), 1416, doi:10.1029/2001JA005090.

Abel, G. A., A. N. Fazakerley, and A. D. Johnstone (2002b), Statistical distributions of field-aligned electron events in the near equatorial magnetosphere observed by the Low Energy Plasma Analyzer on CRRES, *J. Geophys. Res.*, *107*(A11), 1393, doi:10.1029/2001JA005073.

Anderson, B. J., H. Korth, C. L. Waters, D. L. Green, and P. Stauning (2008), Statistical Birkeland current distributions from magnetic field observations by the Iridium constellation, *Ann. Geophys.*, *26*, 671–687.

Ashour-Abdalla, M., and C. F. Kennel (1978), Nonconvective and convective electron cyclotron harmonic instabilities, *J. Geophys. Res.*, *83*, 1531–1543.

Cattell, C., J. Dombeck, W. Yusof, C. Carlson, and J. McFadden (2004), FAST observations of the solar illumination dependence of upflowing electron beams in the auroral zone, *J. Geophys. Res.*, *109*, A02209, doi:10.1029/2003JA010075.

Horne, R. B. (1989), Path-integrated growth of electrostatic waves: The generation of terrestrial myriametric radiation, *J. Geophys. Res.*, *94*, 8895–8909.

Horne, R. B., and R. M. Thorne (2000), Electron pitch angle diffusion by electrostatic electron cyclotron harmonic waves: The origin of pancake distributions, *J. Geophys. Res.*, *105*, 5391–5402.

Horne, R. B., P. J. Christiansen, M. P. Gough, K. Rönnmark, J. F. E. Johnson, J. Sojka, and G. L. Wrenn (1981), Amplitude variations of electron cyclotron harmonic waves, *Nature*, *294*, 338–340, doi:10.1038/294338a0.

Horne, R. B., R. M. Thorne, S. A. Glauert, N. P. Meredith, D. Pokhotelov, and O. Santolík (2007), Electron acceleration in the Van Allen radiation belts by fast magnetosonic waves, *Geophys. Res. Lett.*, *34*, L17107, doi:10.1029/2007GL030267.

Hubbard, R. F., and T. J. Birmingham (1978), Electrostatic emissions between electron gyroharmonics in the outer magnetosphere, *J. Geophys. Res.*, *83*, 4837–4850.

Iijima, T., and T. A. Potemra (1978), Large-scale characteristics of field-aligned currents associated with substorms, *J. Geophys. Res.*, *83*, 599–615.

Kennel, C. F., F. L. Scarf, R. W. Fredricks, J. H. Mcghee, and F. V. Coroniti (1970), VLF electric field observations in the inner magnetosphere, *J. Geophys. Res.*, *75*, 6136–6152.

Lin, C. S., B. Mauk, G. K. Parks, S. DeForest, and C. E. McIlwain (1979), Temperature characteristics of electron beams and ambient particles, *J. Geophys. Res.*, *84*, 2651–2654.

Lin, C. S., J. l. Burch, S. D. Shawhan, and D. A. Gurnett (1984), Correlation of auroral hiss and upward electron beams near the polar cusp, *J. Geophys. Res.*, *89*, 925–935.

Lyons, L. R. (1974), Electron diffusion driven by magnetospheric electrostatic waves, *J. Geophys. Res.*, *79*, 575–580.
Meredith, N. P., A. D. Johnstone, R. B. Horne, and R. R. Anderson (2000), The temporal evolution of electron distributions and associated wave activity following substorm injections in the inner magnetosphere, *J. Geophys. Res.*, *105*, 12,907–12,917, doi:10.1029/2000JA900010.
Meredith, N. P., R. B. Horne, R. M. Thorne, D. Summers, and R. R. Anderson (2004), Substorm dependence of plasmaspheric hiss, *J. Geophys. Res.*, *109*, A06209, doi:10.1029/2004JA010387.
Ni, B., R. M. Thorne, R. B. Horne, N. P. Meredith, Y. Y. Shprits, L. Chen, and W. Li (2011), Resonant scattering of plasma sheet electrons leading to diffuse auroral precipitation: 1. Evaluation for electrostatic electron cyclotron harmonic waves, *J. Geophys. Res.*, *116*, A04218, doi:10.1029/2010JA016232.
Paranicas, C., W. J. Hughes, H. J. Singer, and R. R. Anderson (1992), Banded electrostatic emissions observed by the CRRES plasma wave experiment, *J. Geophys. Res.*, *97*, 13,889–13,898.
Rönnmark, K., and P. J. Christiansen (1981), Dayside electron cyclotron harmonic emissions, *Nature*, *294*, 335–338.
Rymer, A. M., B. H. Mauk, T. W. Hill, C. Paranicas, D. G. Mitchell, A. J. Coates, and D. T. Young (2008), Electron circulation in Saturns magnetosphere, *J. Geophys. Res.*, *113*, A01201, doi:10.1029/2007JA012589.
Thorne, R. M., B. Ni, X. Tao, R. B. Horne, and N. P. Meredith (2010), Scattering by chorus waves as the dominant cause of diffuse auroral precipitation, *Nature*, *467*, 943–946, doi:10.1038/nature09467.
Tokar, R. L., and S. P. Gary (1984), Electrostatic hiss and the beam driven electron acoustic instability in the dayside polar cusp, *Geophys. Res. Lett.*, *11*, 1180–1183, doi:10.1029/GL011i012p01180.